Electronic Supplementary Information

Sustainable and Recyclable Ionogels for Ionic Thermoelectric Supercapacitor Application

Yu-Syuan Jheng,[a] Ling-Chieh Lee,[a] Shao-Huan Hong,[a] Ching-Chieh Hsu,[a] Qing-Bao Zheng,[a] Chia-Hsin Wang,[b] U-Ser Jeng,[b] Shih-Huang Tung[c] and Cheng-Liang Liu[a,c,d]*

a. *Department of Materials Science and Engineering, National Taiwan University, Taipei 10617, Taiwan.*
b. *National Synchrotron Radiation Research Center, Hsinchu 30076, Taiwan.*
c. *Institute of Polymer Science and Engineering, National Taiwan University, Taipei 10617, Taiwan.*
d. *Advanced Research Center for Green Materials Science and Technology, National Taiwan University, Taipei 10617, Taiwan.*

Characterization

Fourier transform infrared spectroscopy (FTIR) was performed using a PerkinElmer Spectrum Two FT-IR L16000 instrument to monitor the changes in the polymer upon the incorporation of $CaCl_2$. Prior to SEM imaging, the ionogels were rapidly frozen using dry ice and then sectioned with a blade to prepare cross-sectional samples. The freeze-dried ionogels were subsequently examined for their morphologies using a Hitachi S-4800 field emission scanning electron microscope (FE-SEM) operated at an accelerating voltage of 3 kV. Rheological properties were assessed using a TA Instruments HR-2 rheometer, with the temperature range set between 20 °C and 50 °C. For the evaluation of mechanical properties, the samples were meticulously cut into a dog-bone shape, with a gauge section of 2 mm^2 and a length of 17 mm. The tensile tests were performed at a rate of 5 mm min^{-1} using a universal testing machine (EZ-Test, SHIMADZU). Small-angle X-ray scattering (SAXS) and X-ray photoelectron spectroscopy (XPS) measurements were conducted at the National Synchrotron Radiation Research Center (NSRRC) in Taiwan. These analyses utilized Beamline TPS 13A1 for SAXS and Beamline TLS 24A1 for XPS, respectively, focusing on a localized region of the ionogel surface to provide detailed insights into its structural and compositional characteristics. The XPS analysis was conducted in an ultra-high vacuum environment to ensure precise measurements. Thermogravimetric analysis (TGA) was performed using a TA Instruments Q500 system, with the temperature range set between 20 °C and 450 °C. This technique involves a stepwise heating process to determine the thermal properties of the materials. The decomposition temperature (T_d) is defined as the temperature at which a 5% weight loss occurs.[1, 2]

Table S1 Composition parameters of the sample.

Sample	LA [mg]	HPC [mg]	AA [µl]	BMIM:Cl [mg]	$CaCl_2$ [mg]
LACG	1000	60	200	0	0
LACIG-0%	1000	60	200	300	0
LACIG-1%	1000	60	200	300	10
LACIG-2%	1000	60	200	300	20
LACIG-3%	1000	60	200	300	30
LACIG-4%	1000	60	200	300	40
LACIG-5%	1000	60	200	300	50

Table S2 The slope and characteristic length derived from the Bragg relationship were employed to analyze the SAXS data obtained from LACIG-X%.

Sample	|Slope|	*d* [Å]
LACIG-0%	2.5	25.1
LACIG-1%	2.4	27.1
LACIG-2%	2.4	27.4
LACIG-3%	2.4	27.9
LACIG-4%	2.3	30.2
LACIG-5%	2.3	32.9

Table S3 A summary of the thermoelectric properties and recyclability of representive i-TE materials.

Materials	Thermopower [mV K^{-1}]	Power Factor [mW m^{-1} K^{-2}]	ZT_i	Recyclability	Ref.
PVDF-HFP/EMIM:TFSI	−4.00	0.003	0.007	No	[3]
ZI copolymer/EMIM:TFSI	−5.40	0.014	N/A	No	[4]
PEO/LiTFSI/EMIM:BF_4	−15.00	0.037	N/A	Yes	[5]
Cellulose/AMIM:Cl/ZnCl	−3.06	N/A	0.100	Yes	[6]
PVDF-HFP/NaTFSI/PC	−6.00	N/A	0.200	No	[7]
PVDF-HFP/NaTFSI/PC	−10.20	N/A	N/A	No	[8]
Cellulose/BMIM:Cl/$CaCl_2$	−30.40	0.024	0.037	Yes	This work

Table S4 Statistical parameters related to the thermoelectric properties of the LACIG-X%.

Sample	Thermopower [mV K^{-1}]	Ionic Conductivity [mS cm^{-1}]	Thermal Conductivity [W $m^{-1} K^{-1}$]	ZT_i [$\times 10^{-3}$]
LACIG-0%	−12.7 ± 1.48	0.07 ± 0.004	0.176 ± 0.0008	2 ± 0.4
LACIG-1%	−19.8 ± 0.72	0.13 ± 0.003	0.179 ± 0.0007	9 ± 0.6
LACIG-2%	−23.0 ± 0.52	0.22 ± 0.005	0.183 ± 0.0006	19 ± 0.8
LACIG-3%	−30.4 ± 0.59	0.26 ± 0.002	0.189 ± 0.0011	37 ±1.5
LACIG-4%	−27.0 ± 0.98	0.30 ± 0.002	0.192 ± 0.0008	34 ±2.5
LACIG-5%	−25.8 ± 0.68	0.35 ± 0.003	0.195 ± 0.0006	35 ±1.8

Table S5 Decomposition temperature (T_d) of the LACIG-X% samples obtained from TGA analysis.

Sample	T_d [°C]
LACIG-0%	205.5
LACIG-1%	194.2
LACIG-2%	192.1
LACIG-3%	191.6
LACIG-4%	184.7
LACIG-5%	181.5
REC-LACIG-3%	190.0

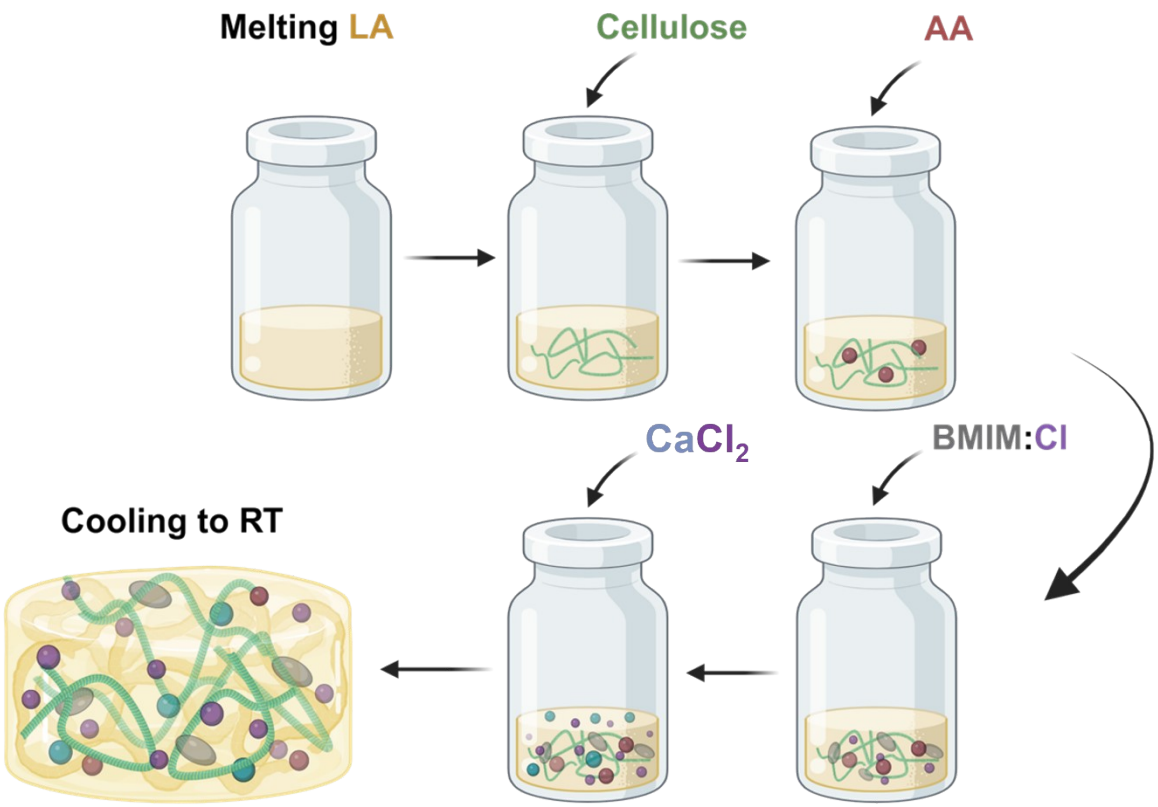

Fig. S1 Diagram illustrating the experimental procedure for the fabrication of the LACIG-X%.

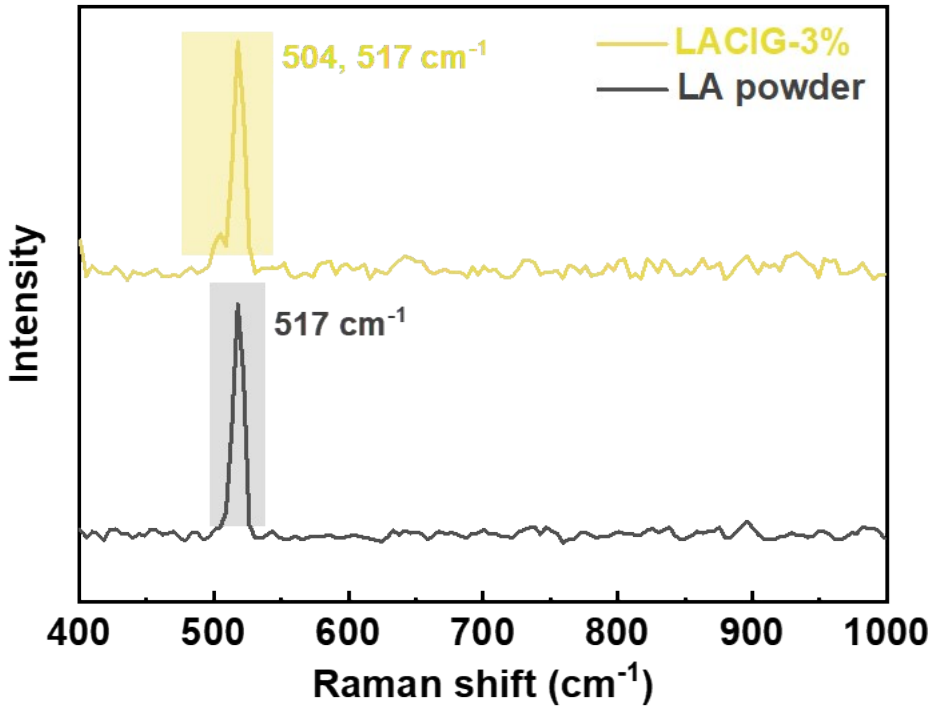

Fig. S2 Raman spectra of LA powder and LACIG-3%.

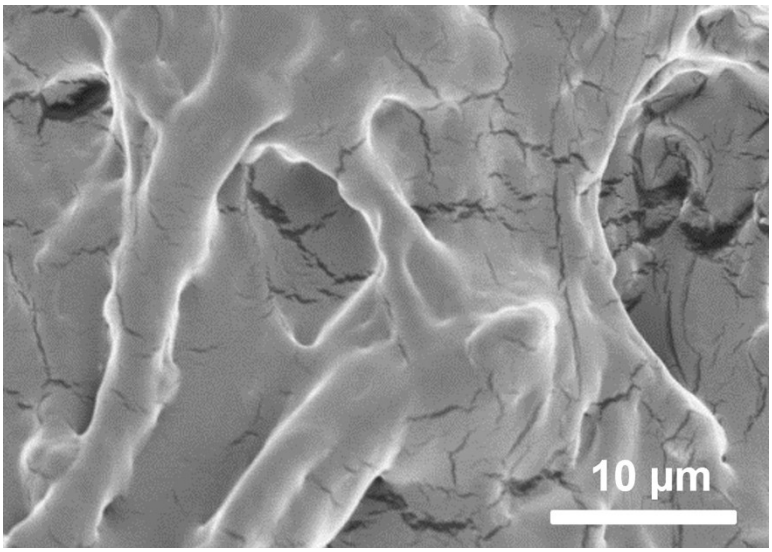

Fig. S3 The SEM images of the gel composed of LACG.

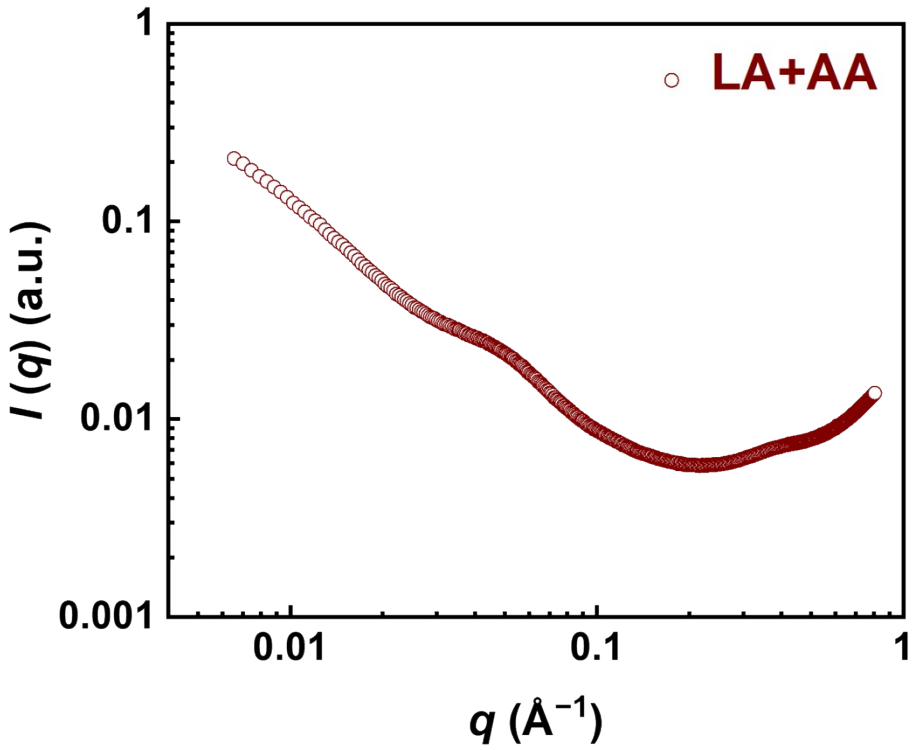

Fig. S4 SAXS patterns for the gel synthesized from LA and AA at 25 °C.

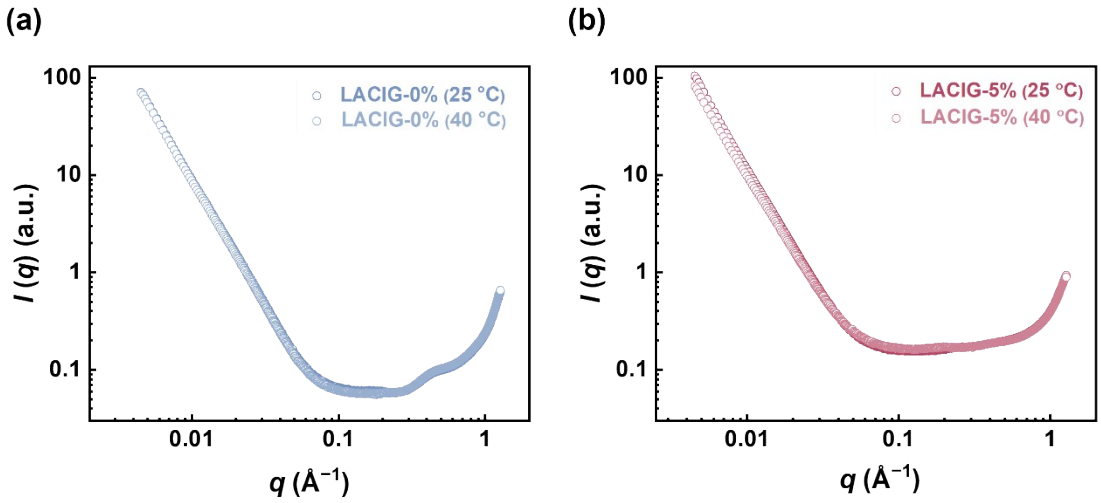

Fig. S5 SAXS patterns for (a) LACIG-0% and (b) LACIG-5% at 25 °C and 40 °C.

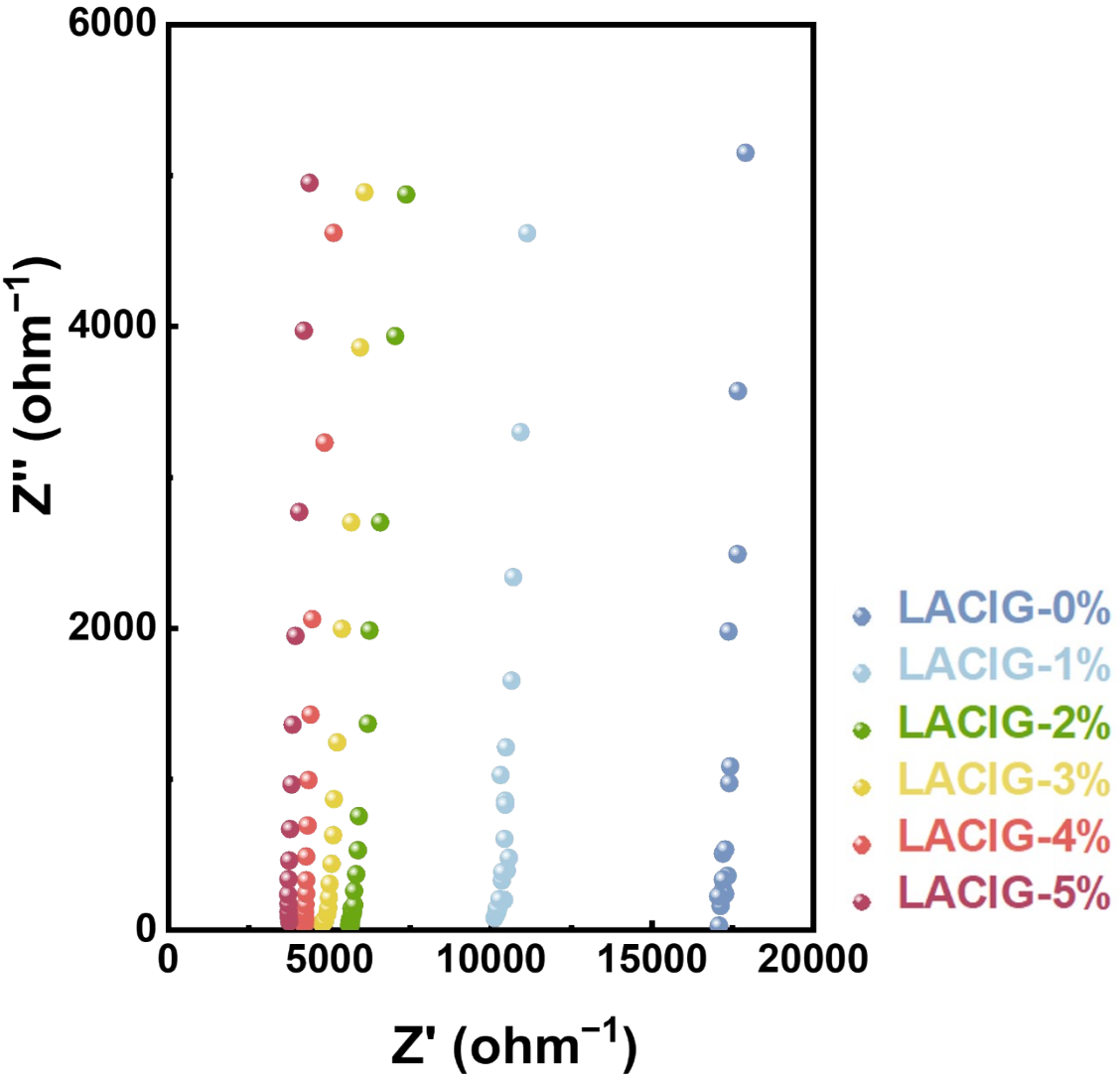

Fig. S6 Nyquist plots from EIS analysis for the LACIG-X%.

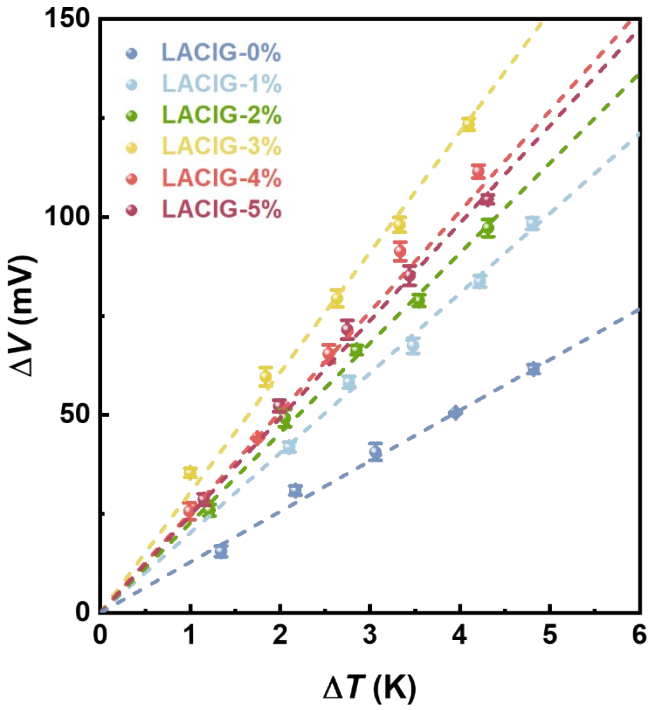

Fig. S7 Δ*V*-Δ*T* plot for all LACIG-X% ionogels.

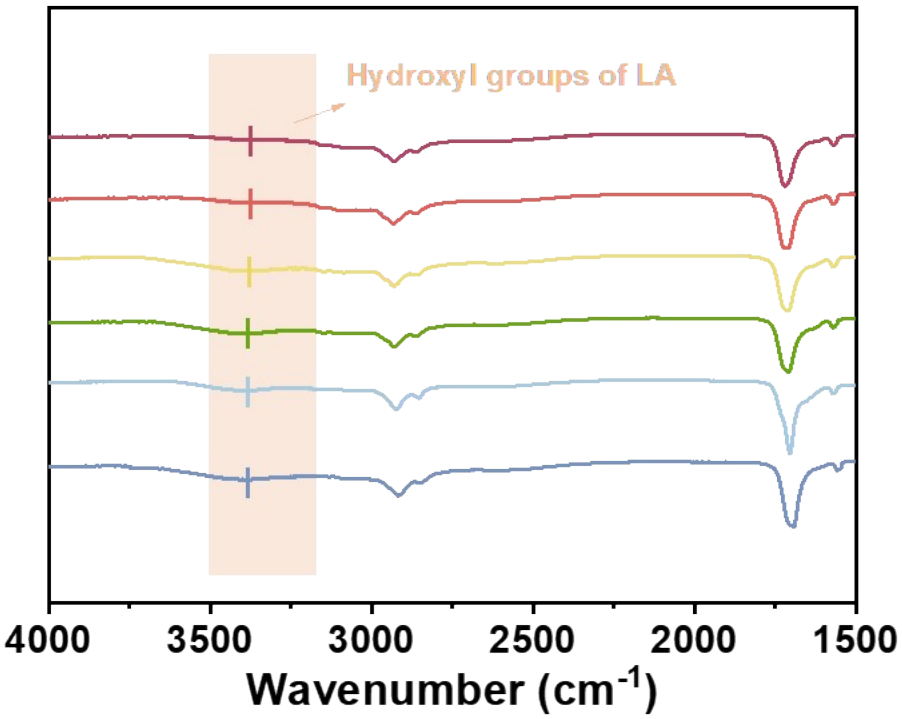

Fig. S8 The FTIR spectrum of LACIG-X% from 4000 to 1500 cm^{-1}.

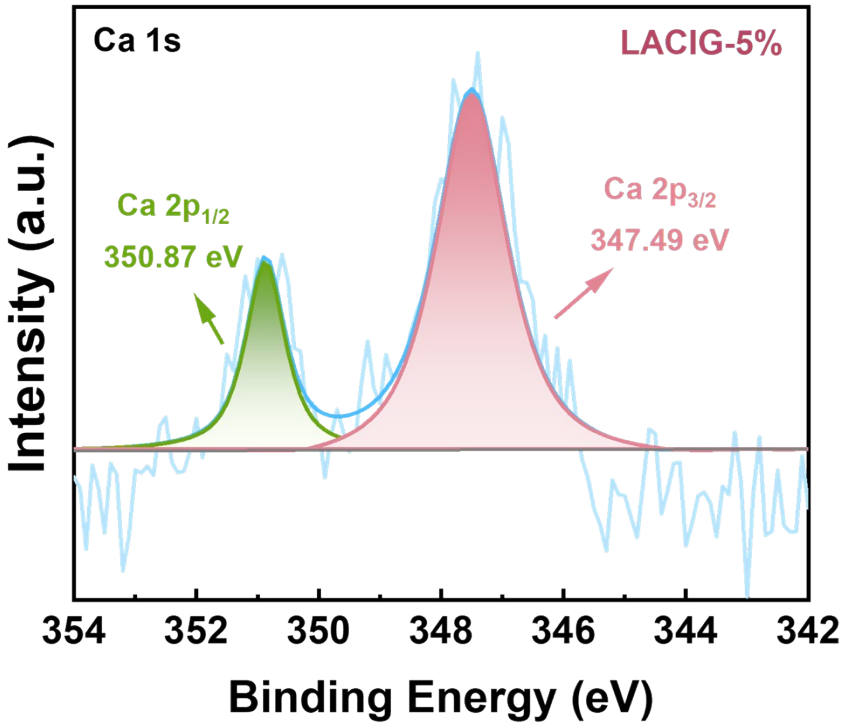

Fig. S9 Ca 2p peak of LACIG-5% in the XPS spectrum.

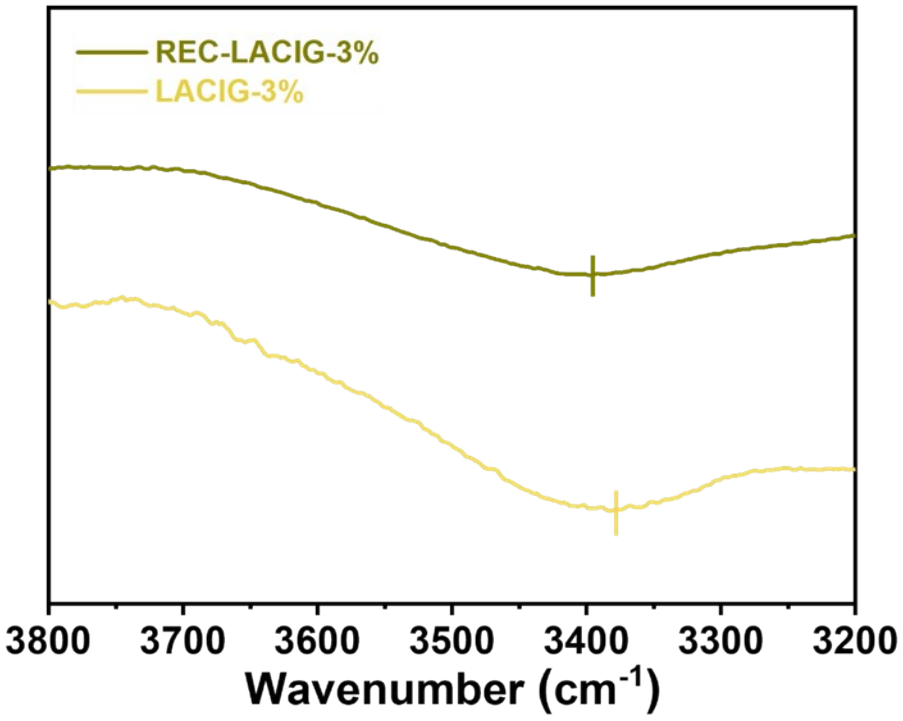

Fig. S10 The FTIR spectrum of REC-LACIG-3% and LACIG-3% from 3800 to 3200 cm^{-1}.

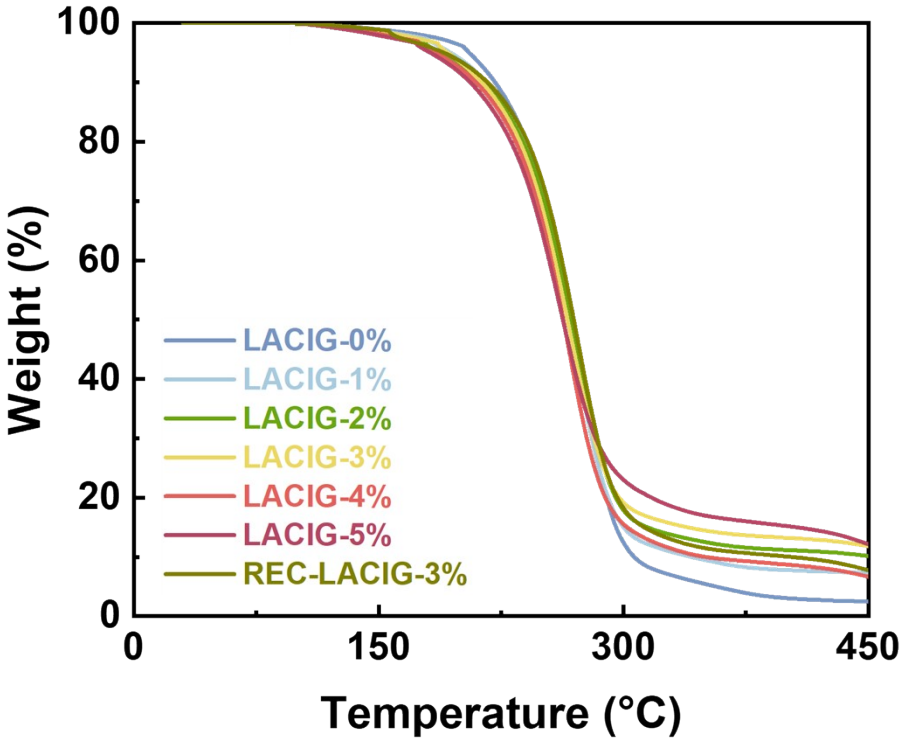

Fig. S11 TGA curves of the LACIG-X% and REC-LACIG-3%.

Video S1 The heating (165 °C, 20 min) and cooling (RT, 1 h) process of the ionogel.

Reference

1. S. Diez, A. Hoefling, P. Theato and W. Pauer, *Polymers*, 2017, **9**, 59.
2. X. Liu, S. Lv, J. Tang, D. Long, Q. Yuan and F. Huang, *Thermochim. Acta*, 2023, **724**, 179489.
3. D. Zhao, A. Martinelli, A. Willfahrt, T. Fischer, D. Bernin, Z. U. Khan, M. Shahi, J. Brill, M. P. Jonsson, S. Fabiano and X. Crispin, *Nat. Commun.*, 2019, **10**, 1093.
4. D. H. Ho, Y. M. Kim, U. J. Kim, K. S. Yu, J. H. Kwon, H. C. Moon and J. H. Cho, *Adv. Energy Mater.*, 2023, **13**, 2301133.
5. W. Zhao, Y. Zheng, M. Jiang, T. Sun, A. Huang, L. Wang, W. Jiang and Q. Zhang, *Sci. Adv.*, **9**, eadk2098.
6. Q. Chen, B. Cheng, Z. Wang, X. Sun, Y. Liu, H. Sun, J. Li, L. Chen, X. Zhu, L. Huang, Y. Ni, M. An and J. Li, *J. Mater. Chem. A*, 2023, **11**, 2145-2154.
7. C. Chi, M. An, X. Qi, Y. Li, R. Zhang, G. Liu, C. Lin, H. Huang, H. Dang, B. Demir, Y. Wang, W. Ma, B. Huang and X. Zhang, *Nat. Commun.*, 2022, **13**, 221.
8. C. Chi, G. Liu, M. An, Y. Zhang, D. Song, X. Qi, C. Zhao, Z. Wang, Y. Du, Z. Lin, Y. Lu, H. Huang, Y. Li, C. Lin, W. Ma, B. Huang, X. Du and X. Zhang, *Nat. Commun.*, 2023, **14**, 306.